

# We are IntechOpen, the world's leading publisher of Open Access books Built by scientists, for scientists

6,900

Open access books available

185,000

International authors and editors

200M

Downloads

Our authors are among the

154

Countries delivered to

TOP 1%

most cited scientists

12.2%

Contributors from top 500 universities



WEB OF SCIENCE™

Selection of our books indexed in the Book Citation Index  
in Web of Science™ Core Collection (BKCI)

Interested in publishing with us?  
Contact [book.department@intechopen.com](mailto:book.department@intechopen.com)

Numbers displayed above are based on latest data collected.  
For more information visit [www.intechopen.com](http://www.intechopen.com)



# Protective Coatings for Magnesium Alloys

Dr. Ing. Stephen Abela

*University of Malta, Department of Metallurgy and Materials Engineering  
Malta*

## 1. Introduction

In the past two decades considerable effort was dedicated to the development of a series of low temperature Physical Vapour Deposition (PVD) techniques suitable for the protection of magnesium alloys. Only a handful of the developed technologies have produced promising results. Some variants of the Ion beam sputter deposition (IBSD), ion beam assisted deposition (IBAD), and reactive ion beam assisted deposition (RIBAD) are among the most promising, as these allow the deposition of hard and dense protective coatings even at room temperature. In the first part of this chapter, the wear and corrosion properties of the selected coating systems will be presented together with a critical analysis of the work published by the author and selected researchers. This will be followed by a more in depth description of the IBAD and RIBAD process. The effect of the various processing parameters on the coating endurance as well as the surface integrity of the substrate materials will be discussed. The relative wear resistance to the pin on disc wear test will be presented and discussed in the light of various experimental evidence collected by the author over the years. This will be followed by a description of a series of test conducted to establish the effectiveness of various coatings in protecting the substrate from electrochemical corrosion in acidified NaCl solutions. The chapter will be concluded with an overview of the current state of PVD technologies with particular emphasis on the strengths and limitations of the existent technology as far as the treatment of light alloys is concerned. Based on the acquired knowledge, the author will endeavour in a discussion of the future trends in PVD and plasma surface modification technologies. A handful of innovative processes and some preliminary results will be included.

## 2. Background

At the December 1997 Kyoto Conference on climate change, more than 159 countries undertook to reduce their emissions of a group of greenhouse gases, by 8% during the period 2008 to 2012 relative to 1990 levels. In response to this commitment, the European Parliament approved Council Directive 1999/94/EC of the 13<sup>th</sup> December 1999, related to the availability of consumer information on fuel economy and CO<sub>2</sub> emissions, in respect of the marketing of new passenger cars. In 2007 EU leaders endorsed an integrated approach to climate and energy policy and committed to transforming Europe into a highly energy-efficient, low carbon economy. They made a unilateral commitment that Europe would cut

its emissions by at least 20% of 1990 levels by 2020. This commitment is being implemented through a package of binding legislations. In addition to these already stringent measures, the EU has offered to increase its emissions reduction to 30% by 2020, on the condition that other major emitting countries in the developed and developing worlds commit to do their fair share under a future global climate agreement. This agreement should take effect at the start of 2013 when the Kyoto Protocol's first commitment period will have expired. Across the Atlantic, Senator John Kerry (D-MA) pushed legislation to raise the current Corporate Average Fuel Economy (CAFE) standards to 37 miles per gallon, up from the current 27.5 mpg for passenger cars, and 20.7 mpg for light trucks.

In order to abide to the new regulations and be competitive, automobile manufacturers must find ways and means to reduce the fuel consumption of the vehicles they produce. Apart from automobile, the attainment of these energy consumption targets would invariably involve weight reduction in a myriad of other mobile equipment and products. To mention just a few: aeroplanes, space vehicles, cargo containers, various tools and fixtures which has to be transported from site to site, sports and accessibility equipment, ships, suit cases, and the list goes on. There are various ways in which this weight reduction can be accomplished. Often these modifications almost always involve the use of stronger and / or lighter materials.

Magnesium offers a set of highly attractive properties for the manufacturing industry. The most obvious of which is magnesium's low density, but there are many more. Magnesium has a low specific heat capacity namely 1025 J/KgK and a relatively low latent heat of fusion 368 KJ/Kg; both properties desirable for all sort of casting processes resulting in a significant reduction in energy consumption in its processing. Moreover, this element has a low affinity to steel. Due to this property, steel moulding tools used for the casting of magnesium alloys, last three to four times longer than those used to cast aluminium. Other attractive properties are excellent castability, high dimensional stability, easily predictable shrinkage, high strength-to-weight ratio, low melting temperature, shock and dent resistance, excellent damping properties [1], practically transparent to high energy neutron radiation, and good electromagnetic shielding [2]. Magnesium is abundant. It is the eighth most common element; seawater, the main source of supply, contains 0.13% Mg, which represents a virtually unlimited supply. Magnesium is also recyclable, and instituting a recycling system would extend supplies and save energy.

In the past the use of these versatile materials has been hindered by their prominent tendency to staining and corrosion in wet and salt-laden atmospheres [3]. On top of this, their poor wear resistance considerably limits the applicable contact loads. These two significant limitations were the culprits for the initial setback for the use of magnesium alloys.

For many years, RZ5 alloy has been the preferred material for helicopter transmission casings due to the combination of low density and good mechanical properties. More recently, however, the requirement for longer intervals between overhauls and hence improved corrosion properties has caused manufacturers to reconsider material choice. In an effort to mitigate this problem WE43 was introduced instead of RZ5 for various components including the main rotor gearbox castings.

In automobile applications the penetration of magnesium was not so successful following the significant setback of the late 60's. Magnesium alloys are currently used in relatively small quantities for auto parts, generally limited to die casting. Studies conducted at the

Argonne National Laboratory, Transportation Technology R&D Centre investigated the use of magnesium sheet in non-structural and semi-structural body applications and the use of extrusions for structural applications as spaceframes, L. Gaines et. al. [4]. This study identifies high cost as the major barrier to greatly increased magnesium use in automobile. In Europe, the increase in using magnesium as a structural lightweight material is being led by the Volkswagen Group of companies, with the material also being used by other leading manufacturers including DaimlerChrysler (Mercedes Benz), BMW, Ford and Jaguar. Presently, around 14kgs of magnesium are used in the VW Passat, Audi A4 & A6. All those vehicles use magnesium transmission casings cast in AZ91D, offering a 20%-25% weight saving over aluminium. Other applications include instrument panels, seat frames, intake manifolds, cylinder head covers, inner boot lid sections, steering wheels, and steering components which utilise the more ductile AM50A & AM60B alloys. In North America, the use of magnesium for auto applications is more advanced. The GM full sized Savana & Express vans use up to 26kg of magnesium alloy. Several Technical barriers remain inhibiting the high-volume uptake of Mg in the automobile industry, galvanic corrosion being second only to the economical issues.

The application of durable anodic or conversion coatings typically provides moderate protection. Anodic coatings such as Keronite™, Magnellan™, and Thixomat™ are tougher and offer better protection from wear and corrosion than conversion coatings, but their cost is too high for the mass production of common goods. Chromate-based conversion coatings are cheaper, but the hexavalent chromium ion involved in this process is both carcinogenic and a hazardous air pollutant. Directive 2000/53/EC on end-of-life vehicles makes explicit reference to the reduction or elimination of its use in cars. Other European regulations are also in place, to control the disposal of process waste and to protect staff in the workplace which could potentially limit the use of such treatments.

The relatively low intrinsic hardness of magnesium and its alloys makes them prone to mechanical damage (wear). In practice, magnesium alloys are protected either by the use of bushings and various metallic inserts. This, however, often leads to galvanic corrosion problems, and require complex and expensive assemblies in order to minimize contact corrosion. It can therefore be safely concluded that the main technological disadvantages of magnesium with respect to other competing materials (mainly plastic, wood, and aluminium alloys) are the poor corrosion and tribological properties.

One of the most important goals for the automotive industry of the future is to extend the use of Mg alloys to other bulky components of the car including external parts such as frames and panels [4], [5]. For active components applications, such as pistons, cylinder blocks, and turbine components, both erosion and corrosion resistance are mandatory if magnesium alloys are to be successfully used. Wear and corrosion protective coating system for magnesium alloys are required in order to unlock the full potential of this virtually inexhaustible recourse. Ideally such coatings would allow the design of magnesium components without bearing inserts and the need of complex fixtures intended to electrically isolate the components from other materials. Reducing the risk of galvanic corrosion by means of a suitable protective coating would therefore result in an overall reduction in production costs and increased reliability. These protective systems have to be compatible with modern magnesium alloys as well as the environment. This can only be achieved if the effect of the required processing parameters on the substrate material is well understood. Also the process itself and the applied coating systems have to be

environmentally friendly, both in terms of energy consumption as well as emissions in the environment during the entire product lifecycle.

### 3. Surface engineering of magnesium alloys

Associated with the ever-increasing need for efficiency and better performing engineering components, there is a corresponding increase in the demands placed on engineering materials. Materials need to be strong, hard, light, ductile, wear resistant, corrosion resistant and aesthetically attractive. Indeed, for some applications, even specific magnetic and optical properties are also required; this is particularly true for the electrical and electronic industry. It is therefore, becoming increasingly difficult for any material, to satisfy all the requirements for a particular application.

Surface engineering enables the modification of the material's surface without drastically affecting the properties of its bulk. This emerging branch of engineering was defined by the late Professor Tom Bell [6] as... *"Surface engineering is the application of traditional and innovative surface technology to engineer components and material, in order to produce a composite material with properties unattainable in either the base or the surface material"*. With these new techniques, it is possible to select a material for its bulk properties, and afterwards engineer its surface to achieve the required set of properties [7]. Surface modification techniques can be tailored to satisfy the requirements of specific class of materials. In the case of magnesium alloys this involves the development of low temperature processing techniques which can modify the surface without degrading the properties of the bulk material.

Surface treatments are primarily applied to magnesium parts to improve their appearance and corrosion resistance [1 pg.143-161]. The selected surface treatments are dependent on the service conditions, aesthetics, alloy composition, size, and the shape of the component to be treated. In the past couple of decades, a large number of surface treatments were developed for magnesium and its alloys, but only few processes have actually achieved commercial importance. The coatings and surface treatments used in industry to protect magnesium alloys are:

- Oils and waxes: *used for temporary protection.*
- Chemical-conversion coatings: *temporary protection or paint base.*
- Anodized coatings: *wear resistance as well as a superior paint base.*
- Paints and powder coatings: *corrosion protection and appearance.*
- Metallic plating: *appearance, surface conductivity, solderability and limited corrosion protection.*

The available surface treatments and coatings offer a wide range of performance and processing cost. Chemical conversion coatings, for instance, can provide limited stand-alone protection for interior environment applications. Anodised coatings are inherently porous, and unless they are properly sealed with paint or resin, are not suitable for exposure to corrosive environments. Metallic coatings are restricted to special applications, because of the high processing costs involved in deposition. Table 1 includes a list of magnesium alloys components, their exposure conditions and the applied surface treatment [1 pg.139].

#### 3.1 Chemical conversion treatments

Chemical conversion treatments are, by far, the most common and diverse surface treatments for magnesium alloys. These treatments are sometimes used on their own, but



Part	Form	Requirement	Pre-treatment	Finish
<i>Automotive parts</i>				
Under hood parts (valve covers, fuel induction housing)	Die cast	Appearance, durability, resistance to salt splash, oils	Wet abrasion or alkaline clean plus chrome-pickle or ion phosphate	Epoxy or epoxy- polyester powder coat
Power-train components (clutch housings, transfer cases)	Die cast	Resistance to salt splash	None	None
Engine brackets and	Die cast	Resistance to heat, salt splash, oils	Wet abrasion of none	None
Wheels	Die cast	Appearance, resistance to UV exposure, , brake dust, stone chipping, humidity	Chrome pickle or ion phosphate	E-coat, TGIC(a) polyester powder and acrylic powder clear coat
Interior parts (hidden items)	Die cast	Humidity	Cut wire aluminium blast, wire brush or none	None
Exterior parts (visible items)	Die cast	Appearance, resistance to weather, resistance to stone chipping, salt splash, UV, break dust	Chrome-pickle or ion phosphate	E-coat, liquid acrylic coat and acrylic powder clear coat
<i>Electronics /computer</i>				
housings	Die cast	Mild interior, sales appeal, durability, adhesion	Chrome pickle or ion phosphate	Sprayed acrylic, polyester or urethane, exterior coating textured epoxy powder coat.
Disc drive activator arm	Die cast / Extruded	Mild interior, limited temperature and humidity variations. No particle release allowed	Dichromate No. 7 or chrome-pickle final dichromate or none on machined surfaces	E-coat on die-cast surfaces, none on extruded surfaces
<i>Aerospace parts</i>				
Aircraft auxiliary components and helicopter gear-box housing	Sand cast	Exterior severe marine and tropical	Sand blast and acid pickle, Dichromate No 7	Backed epoxy primer, polyurethane exterior finish coat or silicate anodize and epoxy coat
<i>Other Parts</i>				
Portable tool housing (chain saws, drillers)	Die cast	Moderate exterior, sales appeal, low cost, adhesion, durability, weather, UV	Wet abrasion and alkaline clean plus chrome pickle or ion phosphate	Modified alkyd or backed alkyd liquid, or electrostatic powder coat with polyester or polyester urethane

Part	Form	Requirement	Pre-treatment	Finish
Compound-archery bow handles	Die cast	Exterior, sales appeal, low cost, adhesion, durability, weather, UV	Chrome pickle or ion phosphate	Electrostatic powder coat with polyester or polyester urethane
Luggage frames	Extruded	Interior plus mild exterior	Chrome pickle or ion phosphate	Clear acrylic
Luggage frames	Die cast	Interior plus mild exterior	Ferric nitrate pickle No 21	Polyester powder coat
Lawnmower decks	Die cast	Moderate exterior	Alkaline clean plus ion phosphate	Polyester powder coat
Photographic plates	Rolled plate	Interior, resistance to wear and corrosion by water based inks on long run painting on can stock	Zincate plus copper strike	Hard chromium electroplate

Table 1. Industrial protection coating techniques for magnesium alloys

most often as surface preparation for subsequent coating. Magnesium metal surface is inherently alkaline and thus its surface must be pre-treated to render it more compatible with paints and other organic coatings in order to enhance adhesion. The protection offered by stand-alone conversion coatings is however limited. This is only sufficient for safeguarding this material during transport and storage. Conversion coatings are also satisfactory for the protection of components intended to operate in relatively mild conditions, such as housing for electronic components and parts for components which are intended for indoor use.

The essential active ingredient in the vast majority of the chemical-conversion treatments of magnesium and its alloys is the hexavalent chromium ion, Cr<sup>6+</sup>. Epidemiological studies have shown that workers employed in chromate production facilities have increased incidences of lung cancer, nasal irritation, atrophy, and nasal septum perforation as well as upper and lower respiratory effects. Chromium-exposed workers are exposed to both the chromium (III) and (VI) compound, but only chromium (VI) has been found to be carcinogenic. Much effort has been dedicated in finding effective substitutes for chromate treatments. Several commercial phosphate treatments, and simple phosphate formulations, emerged in the past decade as paint bases for high purity die-cast alloys, such as the AZ91D, AM50A, AM60B, and AS41B. However, as stand-alone coatings, the original chromate treatment still offer superior corrosion protection, and continues to be the first step in the finishing of many magnesium parts. This is particularly true for components used in severely corrosive environments and sand castings, intended for used in aerospace and military application [3]. The most common conversion coatings used in industry are: the chrome-pickle, Dichromate, Chrome manganese, Ferric nitride pickle, and the phosphate treatments.

3.2 Anodic treatments

Anodic treatments are conducted by applying an electric current to the component being treated, while it is immersed in a specifically formulated anodizing solution. During the process, the component’s surface is forced to react rapidly with the solution, resulting in the

formation of a complex coating, in a number of steps. First the surface of the magnesium alloys forms a thick parent metal oxide. Then, as soon as the dielectric strength of this film reaches the level of the applied impressed voltage, arcing takes place at the metal solution interface. The heat generated by arcing, decomposes chemical precursors in the solution, and results in the concurrent deposition of oxides of other elements. The outcome is a thick and hard coating which significantly modifies the surface properties and favours the adhesion of post-treatment coatings, for example painting [8]. Anodizing treatments require a higher capital investment and have higher running costs, than most chemical conversion coatings. These are also generally environmentally cleaner than chemical conversion processes, despite most formulations in use include fluoride salts [9]. However, the result is a tougher and better supporting paint base, with superior wear resistance. In addition, the porous anodized surface can be infiltrated with organic sealants to give enhanced corrosion resistance in aggressive environments.

Anodised surfaces can be infused with a variety of polymeric substances to produce coatings, having special surface properties, such as lubricity and enhanced paint adhesion. Proprietary coatings of this type are commercially available. One such protection system is an anodic protection film, produced by Thixomat, (Chemical treatment No9 - galvanic anodizing). This treatment is a low voltage dc process, producing a thick black conversion coating, used mainly as a paint base. For rigorous service conditions, such as aerospace applications, thicker coatings can be achieved by using chemical treatment No17 or HAE. These processes can produce coating thicknesses in the range 5-30µm. Thick coatings provide an excellent base for heavy-duty paints and offer significant resistance to abrasion.

### 3.3 Other coatings used for magnesium alloys

Magnesium alloys can be electroplated by many commercial plating systems provided proper pre-plating operations are conducted. However, the only metals which can be plated directly on magnesium are zinc and nickel. Zinc and nickel under-coatings serve as surface preparation for cadmium, copper, brass, nickel, chromium, gold, silver, and rhodium coatings. With the exception of gold plating, metal coatings have found little commercial applications. This is because they offer limited protection against wear and corrosion, and also because of the high processing costs. Gold plating is still used in space applications, because of its extreme stability in all operating environments, resistance to tarnish and radiation, high superficial electrical conductivity, low infrared emissivity, and resistance to cold welding in high vacuum. Metal plated wrought alloys give better and more reproducible corrosion resistance than cast alloys. This has been attributed to the surface porosity found in cast alloys [3].

Organic coatings are used on magnesium alloys to provide corrosion protection and for decoration. Organic finish paints range from single coats applied, on a pre-treated surface, to complex multicoat™ systems involving anodizing, epoxy surface sealing, priming, and one or more topcoats. Surface sealing with epoxy resin was developed, as a first step in the finish of casting for the aerospace and military applications. This sealing is an important step to increase the corrosion performance of the complex finishing systems required in aggressive environments and to seal the inherent surface porosity of cast alloys [3].

### 3.4 Low temperature physical vapour deposition (IBAD)

Plasma processing of materials has matured at an incredible rate. Since the first international conference, on plasma surface engineering, held on the 19-23 September 1988, in Garmisch-



Partenkirchen, the state of technology has made unprecedented strides. As early as 1989, low temperature ion assisted film growth processes, were already predominantly forcing their way for the fabrication of microelectronic devices. Plasma Assisted Physical Vapour Deposition provided a useful way to make the condensable particles move around on the substrate surface by colliding energetic particles from the plasma with those being adsorbed on the surface. This is accomplished by applying a negative potential to the substrate during deposition. In this way the deposition temperature required to achieve relatively dense and hard coatings was steadily reduced lowering energy consumption and reducing the heat input to the substrate during deposition. Heightened environmental concerns, in recent years has made plasma processes increasingly important in the surface engineering of materials.

Ion beam assisted deposition (IBAD), also referred to by some scientist as ion beam enhanced deposition (IBED), is a combination of two surface treatment processes, namely, physical vapour deposition (PVD) and ion implantation [10]. In this case the source of condensable particles and energetic particles are distinct and can be controlled independently. The deposition process is usually accountable for the material build-up, while the ion flux imparts the kinetic energy required to achieve adhesion and the required coating properties [11]. The kinetic energy imparted by the ion beam activates a number of processes on the surface of the growing film. Surface atoms are displaced, enhancing migration of atoms along the surface and thereby increasing the coating density even at very low deposition temperature. The ion beam, also provides the required stitching (ion beam mixing) of the coating to the substrate at a low temperature [12]. This process is therefore applicable to a wider range of materials [13, 14, 15]. Furthermore, accurate tuning of the ion to condensable flux ratio, enables the control of coating stoichiometry, structure, and residual stresses [16].

The main difference between the IBAD deposition technique and other ion assisted deposition processes is that, in the former, the energetic ion source and the condensable material flux source are separated into two distinct devices. Thus in IBAD, these two parameters can be controlled independently. In comparison, other plasma based deposition techniques such as DC and RF magnetron sputtering, as with all other PEPVD techniques, the condensable material and ion fluxes are extracted from the same plasma source. This feature gives the IBAD process more control over the deposition parameters, as compared to other deposition processes [17]. Another important difference is the operating pressure. Plasma assisted coatings usually operate between  $0.1 \times 10^{-2}$  – 13 mbar, which is the pressure required to sustain a plasma. In contrast, IBAD techniques usually operate at high vacuum, between  $2 \times 10^{-6}$  and  $2 \times 10^{-10}$  mbar. This is mainly due to physical limitations of the hardware and mean free path restrictions, R. Emmerich et al. [18]. IBAD techniques operate in the collision free pressure regime, thus the evaporant and the ion beam flux travel in straight lines to the substrate. This is a serious limitation of IBAD process, which restricts the complexity of the parts that can be treated which would otherwise cast shadows on the surface to be coated. This limitation is known as line-of-sight.

Conventional plasma assisted deposition techniques allow for the deposition of coatings with thickness ranging in the tens of microns. However, the interface between the coating and the substrate is often very thin, especially, when the process is conducted at low temperatures. Frequently, this results in poor coating adhesion, particularly for coatings thicker than three microns. Ion beam mixing can potentially solve this problem. In this process, the substrate is coated up to a thickness which is shallower than the penetration

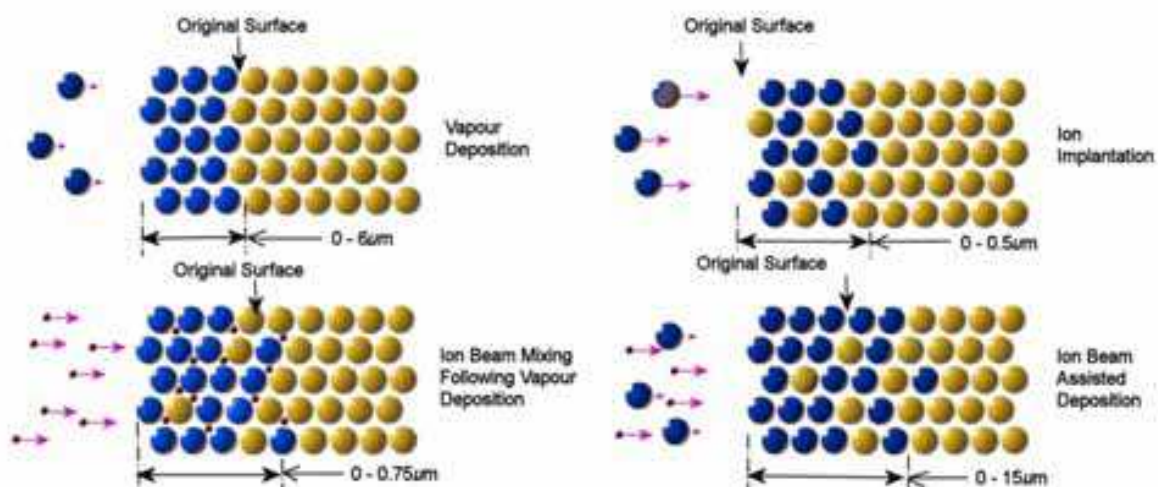


Fig. n.1. Physical vapour deposition processes [19]

depth or the ions. This thickness is dependent on the maximum available ion energy. The newly formed surface is subsequently ion implanted such that, the original interface is broadened by the ballistic effect of the ion beam as shown in figure n.1 [20, 21]. The resulting coating is very shallow, in the range of  $0.2 - 0.5\mu\text{m}$ , but the physical properties are vastly superior to those produced by traditional methods. This shallow coating provides an excellent foundation for additional coatings. By combining ion irradiation and deposition, the IBAD process allows for the deposition of relatively thick coatings sometimes with a thickness of more than  $30\mu\text{m}$  and excellent adhesion to the substrate. In addition, it provides a means to control the residual stresses, as well as, the texture of the coating produced.

There are two principal ways to carry out IBAD process. The coating can be deposited under simultaneous or alternating ion bombardment. In the first case, low energy ion sources with no mass separation are used, such as the broad-beam Kaufman type. In the second case, higher beam energy is required, depending on the thickness deposited between each irradiation intervals, figure n.3. The increment in thickness on each successive pass is, usually, a few tenths of nanometres. In both cases, the typical energy range used for IBAD / RIBAD is  $100\text{eV} - 300\text{eV}$ ,  $30\text{KeV} - 100\text{KeV}$ . When energies higher than a few hundred eV are used, decomposition of the deposited compounds occurs and the coating structure is damaged. This is particularly the case in the RIBAD process [22]. Figure n.2 illustrates a grid array of nano hardness measurement taken from an AM50 magnesium substrate coated with IBAD alumina. For the preparation of these alumina layers the growing alumina film was irradiated with a low intensity flux of  $80\text{KeV Ar}^+$  ions. The hardness values shown in this figure suggest the presence of hard crystalline sapphire crystals in a soft amorphous matrix. The presence of these structures in coatings deposited with different ion beam to condensable flux ration was verified using polarised light, figure n.3.

An alternative method for material deposition commonly in use is the sputtering of condensable material from a solid target, which is situated in front of the substrate. This can be accomplished either by immersing the target in dense plasma and applying a substrate bias or by irradiating the target with a high intensity ion beam with energies in the range  $100\text{eV} - 600\text{eV}$ . The former process is known as magnetron sputtering while the latter process is known as ion beam sputter deposition (IBSD). Magnetron sputtering allows for very high deposition rates but in order to obtain dense coatings higher temperature are

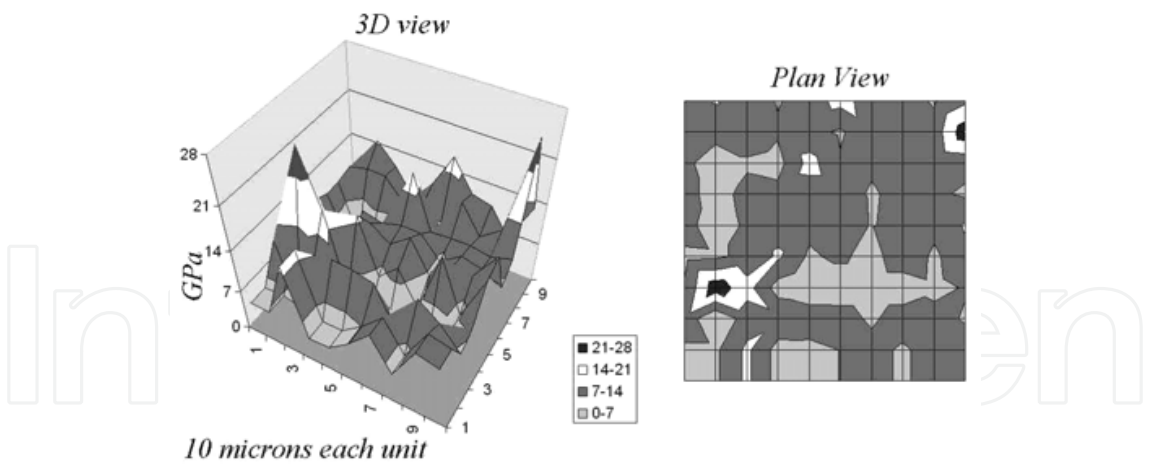


Fig. n.2. Nano hardness measurements on IBAD Al<sub>2</sub>O<sub>3</sub> coating with I/C ratio of 0.3 to determine the hardness of the phases present.

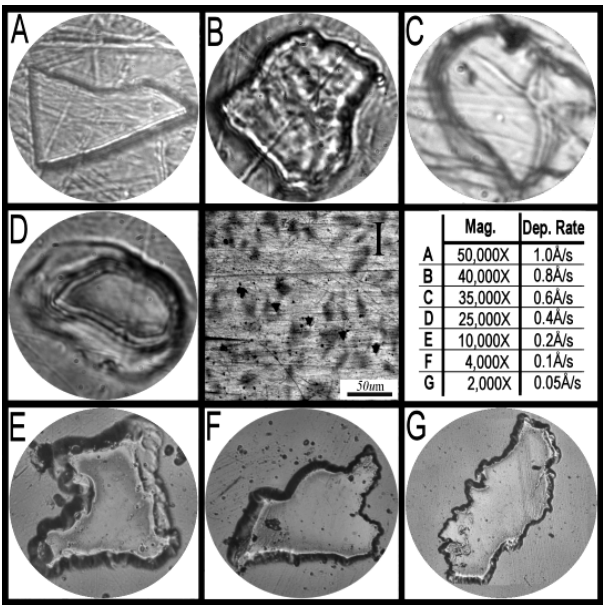


Fig. n.3. Selected areas from a series of IBAD Al<sub>2</sub>O<sub>3</sub> coatings (plate A - D) prepared with different I/C ratios. Plate I at the centre illustrates the distribution of the hard island on the surface along with a series of nano indentations

required. In IBSD, the condensable material sputtered from the target attains very high energies 60eV – 100eV and through self bombardment can yield very dense coatings even at cryogenic temperatures. In the bottom of Figure n.4, a single ion source IBSD setup is illustrated, while the top part of the same figure shows the two ion sources configuration. IBSD sputtering usually result in very low deposition rates and require ultra high vacuum, to limit coating contamination from the residual gas and avoid scattering of the condensable particles by the residual gas particles which would result in inferior mechanical properties. The high kinetic energies of the condensable particles impart excellent adhesion and coating densification resulting in superior wear and corrosion protection, B. Valvoda [23]. It is because of this high kinetic energy, that IBSD can be conducted at lower temperatures than any other physical deposition process [24].

Clearly, the two ion source configuration offers greater flexibility and control over coating structure and stoichiometry [25]. Then again, multiple evaporation and ion sources may be required for the synthesis of compound coatings. A configuration of two separately controlled ion sources has achieved a relative degree of success in the United States. One institution using this system in the early 1980's, was the U.S. Naval research laboratory, which developed a series of processes suitable for high temperature aerospace applications [15].

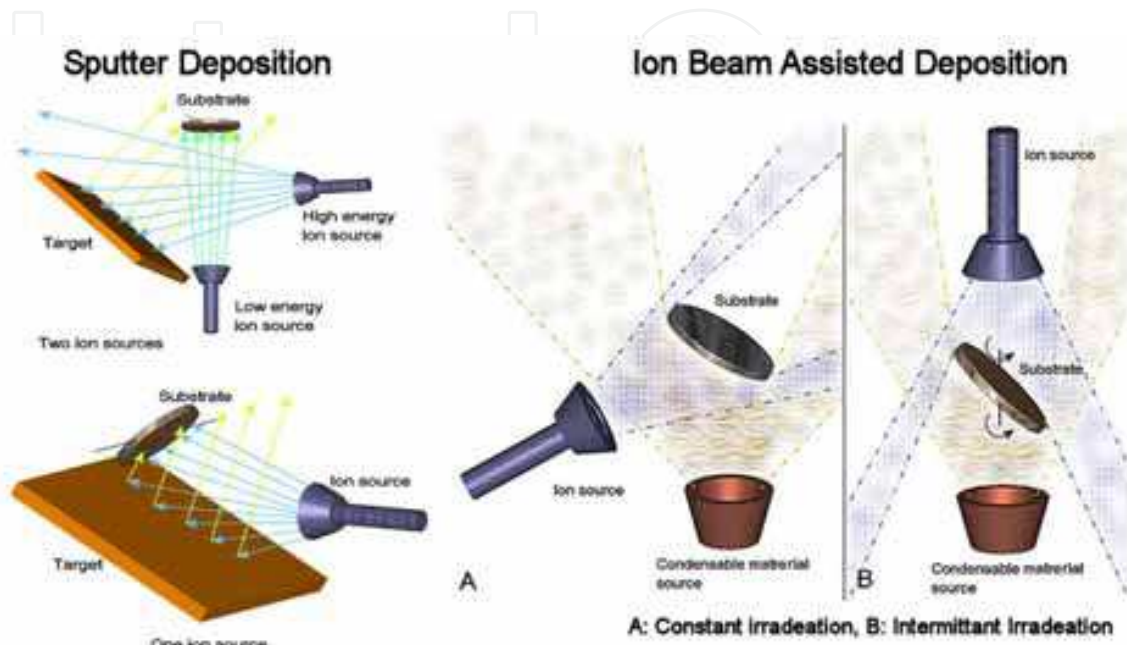


Fig. n.4. Deposition Configuration

### 3.5 Mechanical properties of low temperature PVD coatings for magnesium alloys

The physical properties of the resulting PVD films are extremely sensitive to a broad range deposition parameters used for their preparation. The substrate surface conditions (roughness, hardness, crystal orientation, and density of point defects) and to a larger extent contaminants present on its surface also have a huge impact of such properties. The limited ad-atom mobility at low temperature tends to make films deposit under such condition more sensitive to the presence of contaminants on the substrate surface and relatively high concentration of residual gas molecules in the processing chamber. The effect of the latter is usually more pronounced when the deposition rate is very low (less than  $2\text{\AA s}^{-1}$ ).

As part of an extensive investigation intended to develop protective coatings which could be applied to magnesium alloys in existent industrial deposition facilities, a number of deposition techniques were evaluated. The coatings produced in this investigation were subsequently compared using pin on disk tribo test configuration and various electrochemical tests. The base pressure of the equipment available in this case was  $2 \times 10^{-6}$  mbar and the deposition temperature for all coatings was maintained below  $80^\circ\text{C}$ . A selection of the physical properties of the coatings obtained from this investigation is included in tables 1 and 2.

Under the investigated conditions, ion beam sputtered aluminium oxide, titanium oxide and carbon, coatings have very high wear rates compared to those of sputtered W and ion beam assisted deposition coatings. The best performing coating is RIBAD TiN, resulting in a wear rate of  $2.51 \times 10^{-12} \text{mm}^3(\text{Nm})^{-1}$ . This is followed by IBAD alumina (I/C 0.3) which resulted in a



wear rate of  $8 \times 10^{-6} \text{ mm}^3(\text{Nm})^{-1}$ . The far right pyramid, in this chart, represents the wear rate of  $1 \mu\text{m}$  sputtered carbon on top of a  $5 \mu\text{m}$  IBAD alumina ( $I/C = 0.3$ ) coating. This composite coating wears at a rate of  $2.8 \times 10^{-7} \text{ mm}^3(\text{Nm})^{-1}$ , and shows, therefore, an improvement over the monolithic IBAD alumina coating.

The poor performance of the IBSD coatings in this investigation is attributable to the high residual gas pressure and the extremely low deposition rates used due to the hardware limitations. The relatively high base pressure results in a continuous build-up of physisorbed gas molecules, on the substrate surface, which hinder coalescence of growing coating islands. This gave rise to a high concentration of nanometric voids inside the growing films. The density these coatings were calculated by measuring the difference in weight of the substrate before and after the deposition process and dividing this quantity by the coating thickness multiplied by the CSA of the substrate. These values are reported in table 2 and provide support the hypothesis that the coatings contain significant nanometric porosity which is invisible to the optical microscope and SEM, figure n.3.6. From this table, it can be seen, that the sputtered coatings have very low hardness. The only exception is the sputter deposition of W, which has a very high hardness, even if the coating density is only 0.8 of the theoretical value. This, is believed to be due, to the difference in mass between the residual gas molecules, [ $\text{H}_2\text{O}$  (18amu),  $\text{O}_2$  (32amu), and nitrogen (28amu)] and that of W (184amu). As a result, W particles lose little kinetic energy during binary collisions with residual gas particles on the substrate surface. Chum Gao *et.al.* [26] used this phenomenon by intentionally increasing the chamber pressure to decrease ad-atom mobility and deposit films with nanometric grains containing nano-voids, thus enhance their magnetic properties.

IBSD $\text{Al}_2\text{O}_3$	IBSD $\text{Ti}_x\text{O}_y$	IBSD C	IBSD W	IBAD $\text{Al}_2\text{O}_3$	RIBAD TiN	RIBAD $\text{Ti}_x\text{O}_y$	IBSD C/IBAD $\text{Al}_2\text{O}_3$
2.97E-02	2.60E-02	1.80E-01	7.25E-04	8.00E-06	2.51E-12	9.20E-04	2.80E-07

Table 2. Wear resistance of various coatings, subjected to the pin-on-disc test, the units used to represent the volume of material removed by the pin are  $\text{mm}^3(\text{Nm})^{-1}$

At room temperature, residual reactive gases occupy the reactive sites of the substrate surface and “act as a source of mechanical stresses to pin grain boundaries and vacancies”. In turn, this results in poorly adherent films, which are either amorphous or have very small grains G. Konczos et. al.[27]. At higher temperature the incorporated gases give rise to mechanical stresses in the coatings, and significantly modify both their electrical and optical properties. The presence of these adsorbed gases can also change the deposition mode from epitaxial to polycrystalline or amorphous, depending on the extent of contamination. The continuous formation of residual gas molecular film on the surface is responsible of atomic shadowing. This, eventually, leads to the formation of nano trenches in the surface, which when covered would give rise to the voids reported.

Despite the high residual gas pressure and the low deposition rate, the coating adhesion and wear resistance, reported by P. I. Ignatenko *et.al.*, for IBSD TiN are significantly better than those of RIBAD TiN deposited by on the same substrates [28]. This appears to be in contrast with the results obtained by the author in whom the deposition of IBSD of TiN resulted in a loosely bound mixture of titanium oxides and nitride, with exceedingly poor mechanical properties. This difference originates mainly from the difference in operating parameters used. In fact, in the research at hand, the substrate temperature was not allowed to exceed



	Density gmm <sup>-3</sup>	Coefficient of friction during wear test	Hardness GPa	Adhesion Nmm <sup>-2</sup> * Max 35Nmm <sup>-2</sup>
IBSD Al <sub>2</sub> O <sub>3</sub>	2.92	0.86	0.44	18.2
IBSD Ti <sub>x</sub> O <sub>y</sub>	2.16	0.68	1.28	12.8
IBSD W	16.3	0.56	33.64	16.25 <sup>2</sup>
IBSD C	1.9	0.095	0.11	2.3 <sup>1</sup>
IBSD C on IBAD Al <sub>2</sub> O <sub>3</sub>	-	0.014	20.85	10.73 <sup>6</sup>
IBAD TiN	5.4	0.21	16-26.8	35 <sup>3,5</sup>
IBAD Ti <sub>x</sub> O <sub>y</sub>	3.85	0.42	8.33	33.5 <sup>5</sup>
IBAD Al <sub>2</sub> O <sub>3</sub>	3.9	0.68	2.4 – 26.5	34.1 <sup>4,5</sup>

Table 3. Mechanical properties of coatings

1. Coating flakes off spontaneously after 5 days of exposure in atmosphere

2. Coating develops visible cracks and pores after 3 weeks of exposure in atmosphere

3. Coating develops blisters after 12- 36 months

4. Partial coating and resin failure
5. Coating delaminates but does not debond

6. Failure of resin-coating bond

7. Resin adhesive strength in tension is 35Nmm<sup>-2</sup>

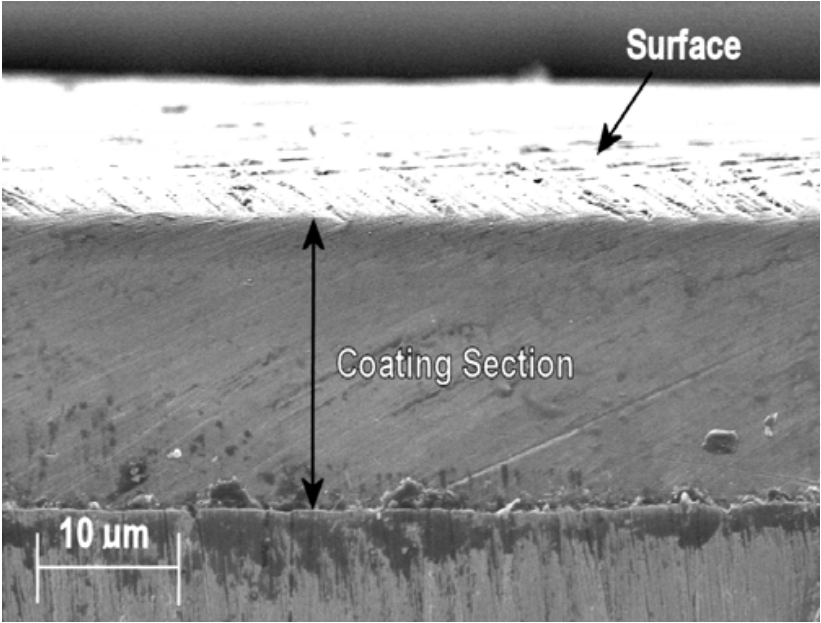


Fig. n.3.6. A sectioned IBSD Al<sub>2</sub>O<sub>3</sub> coating, deposited by sputtering Al with O<sub>2</sub><sup>+</sup> for 432hrs, showing a “thick” and uniform coating

80°C and no substrate bias was used, whilst P. I. Ignatenko *et.al.* applied a deposition temperature of 500°C and a substrate bias of -200V. This is believed to be responsible for the considerable improvement of, both, the coating hardness and adhesion to such an extent that it actually outperformed RIBAD TiN deposited on the same substrate. In fact published

results suggest that under appropriated deposition conditions and with a base pressure in the range of  $1 \times 10^{-10}$  mbar IBSD coatings are generally superior to their counterparts deposited using other PVD techniques.

Results published by I. Petrova *et.al.* show that low density coatings result when metal films are deposited with an impurity arrival rate much higher than that of the metal itself [29]. They also stated that, for alumina deposited under similar conditions, adequate mechanical properties cannot be achieved at deposition temperatures lower than  $500^\circ\text{C}$  in case of ion beam bombardment and  $800^\circ\text{C}$  when no ion beam irradiation is applied. The findings of this investigation concur with the findings of G. Konczos *et.al.*, whose conclusions are based on experimental data gathered from work carried out by a number of researchers, over several decades.

### 3.6 Effect of the surface condition on the low temperature PVD coatings for magnesium alloys

In the deposition of hard coatings on magnesium alloys, magnesium oxide present on the substrate is a weak link and is thought to be responsible for the poor coating adhesion. This oxide is unstable, due to a misfit between the lattices of the cubic oxide and that of the hexagonal metal, resulting in a Pilling-Bedworth factor less than one. In addition, when exposed to humid atmosphere, magnesium oxide reacts to form hydroxide, further compromising coating adhesion, R.S. Busk [30]. While investigating plasma surface treatment of magnesium alloys H. Hoche *et.al.* [31] has shown, that the presence of magnesium oxide, at the interface of a hard coating, is detrimental for the coating hardness and adhesion. They suggest that the weak bond of the MgO, with the parent metal inhibits, the formation of compressive stresses in hard coatings deposited on top of the MgO, resulting in lower hardness and adhesion. This was amply demonstrated in a separate publication by Hoche *et.al.* [32] who report the performance of three coating systems namely  $9\mu\text{m}$  CrN,  $2.1\mu\text{m}$  TiN and  $0.5\mu\text{m}$  anodised Mg +  $3\mu\text{m}$   $\text{Al}_2\text{O}_3$ . In their new setup, they used an RF magnetron source to sputter the condensable material, while feeding the reactive gas. Also, by applying a high substrate bias voltage for 20 minutes, it was possible to remove the surface oxide from the magnesium substrates. Subsequent formation was prevented by gradually reducing the bias voltage and allowing the coating to grow without interrupting the sputtering process. The hardness of the TiN and  $\text{Al}_2\text{O}_3$  coatings deposited with this method is 42.86 GPa and 22.07 GPa respectively. The former is surprisingly higher than the corresponding hardness values of 28 – 34 GPa reported by Jorge Nuno and Marcolino Carvalho [33]. This difference was despite the fact that the substrate in this case was tool steel, with hardness ranging between 50–60 HV.

In a separate investigation the author has demonstrated that because of the marked difference between the atomic weight of magnesium and aluminium atoms and that of zinc, iron, manganese, and zirconium elements which are often present in the most common magnesium alloys, a phenomenon known as sputter amplification is likely to take place during the sputter cleaning of the surface [34]. This process results in the roughening of the surface and the consequent reduction of the coating performance.

Attempts to form stoichiometric MgO on magnesium at reduced pressures and low temperatures ( $0 - 200^\circ\text{C}$ ) in the past has failed, Kurth. M *et.al.* [35]. In their report they described the formation of a nanometric oxide film which is semi conductive, with a band gap of circa 2 eV. In their article they also report that previous attempts to grow thicker MgO layers at elevated temperature, invariably, resulted in cracks in the coating, consequently

leading to poor adhesion and corrosion protection. In contrast, work conducted by F. Stippich *et.al.* has shown that magnesium oxide can be grown, under controlled conditions, to form a protective layer [36]. In their work, they explain that IBAD deposited MgO, using 5-15KeV Ar<sup>+</sup> and an I/C of 0.2, can generate a range of useful crystal structures which can offer moderate corrosion protection on their own, but more importantly can be used to provide support for more protective surface layers.

The intrinsic softness of magnesium and its alloys also contributes to degrade the properties of hard coatings deposited on these materials. In order to minimise this effect, the coating thickness deposited on magnesium alloys has to be substantially greater than that used on harder substrate materials in order to provide adequate protection. The effect of coating thickness on the wear rate of IBAD Al<sub>2</sub>O<sub>3</sub> coating deposited on AM50 substrates was investigated by the author. This investigation uncovered that as the coating thickness is increased, the scatter in wear data becomes less significant and the wear resistance is considerably improved. An interesting result obtained in this investigation was the fact that as the coating thickness was increased from 1µm to 2.5µm there was a corresponding deterioration in wear resistance, figure n.3.7. Increasing the thickness further resulted in the expected rapid improvement. In order to understand the change in the wear mechanism operating on these coatings and explain the initial anomaly, two series of wear tests were carried out. In the first instance, a series of pin-on-disc wear tests were conducted on coatings having thicknesses of 0.85µm, 3.8µm, 5.6µm, & 7µm. In these tests, the pin was allowed to wear through the whole thickness of the coating. In the second set of experiments, the time required for failure of the coating derived from the first set of experiments, was used to determine the duration for two thirds of the coating to be worn off. The results of these tests are given in figures n.3.8 and n.3.9 (pages 149-150).

From figure n.3.8, it can be seen that, for both 0.85µm and 3.8µm thick coatings, the sliding of the pin on the surface results in plastic deformation of the substrate material, leading to a wear process known as gouging. This results in a series of characteristic "V" shaped cracks on the surface of the 3.8µm thick coating pointing towards the sliding direction. Numerous tiny cracks are formed along the edge of the wear track. Interestingly, on the 0.85µm thick coating, no cracks are visible; despite of the extensive plastic deformation of the surface. Both the 5.6µm and the 7µm thick coatings display no sign of plastic deformation or cracking of the surface.

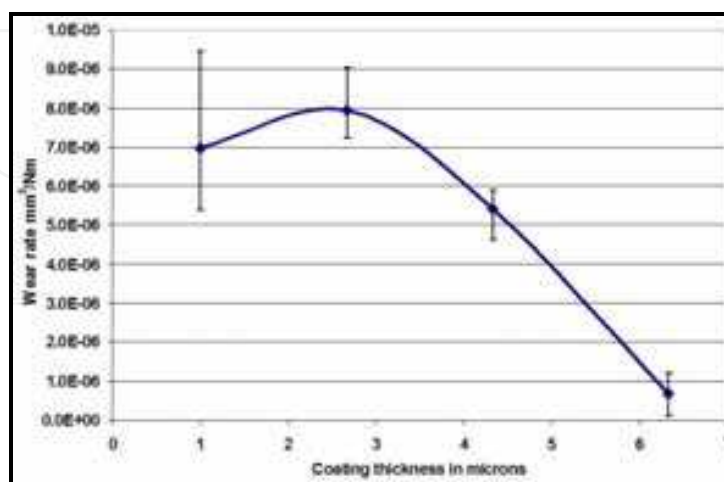


Fig. n.3.7. Effect of coating thickness on the wear rate of IBAD Al<sub>2</sub>O<sub>3</sub> coatings deposited with an I/C ratio of 0.3 and subjected to the pin-on-disc test.

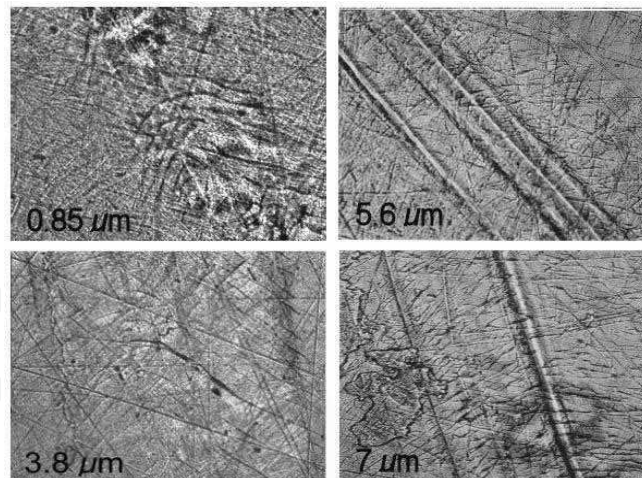


Fig. n.3.8. Optical micrographs of  $\text{Al}_2\text{O}_3$  coatings with different thickness and an I/C ratio of 0.3, showing wear tracks produced by running the pin-on-disc test, for two thirds the time required for the pin to wear through the respective coating

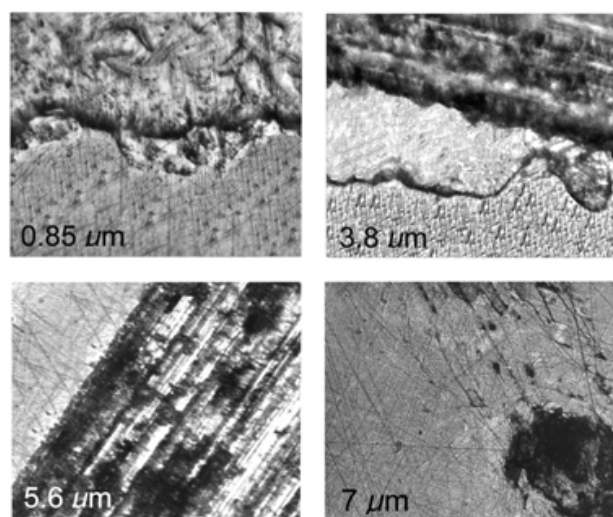


Fig. n.3.9. Optical micrographs of  $\text{Al}_2\text{O}_3$  coatings deposited with an I/C of 0.3 and different coating thickness, showing wear tracks produced by running the pin-on-disc test until failure

Figure n.3.9 indicates that in the case of the  $0.85\mu\text{m}$  thick coating, the cracked coating is still present on the surfaces even when the pin has penetrated substantially in the substrate. It is believed that the plastic behaviour exhibited in this micrograph, is caused by the high magnesium oxide content in the alumina coating, originating from the substrate. EDX measurements show that out of the  $0.84\mu\text{m}$  thick layer a minimum of  $0.4\mu\text{m}$  is actually interphase material having grading chemical composition, figure n.3.10.

The addition of 3-10% magnesium oxide to alumina, significantly, reduces the grain size of sintered alumina [37]. In his clinical trials, H. B. Skinner [38] found, that the reduction in alumina grain size, by alloying with magnesium oxide, resulted in increased wear resistance and toughness of the alumina-bearing surfaces used for hip joint replacement. However, the deformation of the thin coating observed in the present work could simply be due to the shallow thickness of the coating. Reports published by D.R. Clarke and W. Pompe [39] who



investigated the failure of the interface of thin hard coatings subjected to compressive stress, support this second hypothesis. In their findings, they stated that the critical radius for interface separation is inversely proportional to the coating thickness.

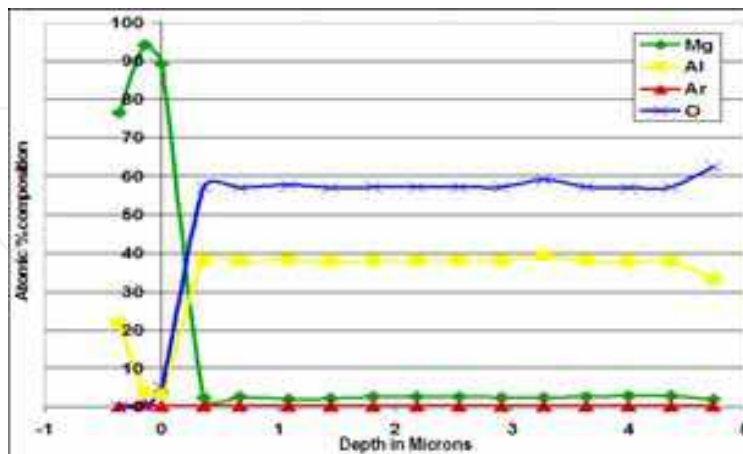


Fig. n.3.10. EDX measurement conducted on sectioned IBAD Al<sub>2</sub>O<sub>3</sub> coating prepared with an I/C of 0.3, showing an interface thickness of 0.6μm

The 3.8μm thick coating, on the other hand, is completely removed from the surface, revealing the microstructure of the AM50 substrate. In fact, figure n.3.9 provides evidence of coating delamination suggesting that at this coating thickness, the shear stress at the interface is too high to provide adequate performance. Increasing the coating thickness to 5.6μm reduces the shear stress at the interface sufficiently; to avoid delamination as can be seen in the same figure. Increasing the coating thickness further to 7μm, results in a substantial improvement in the wear resistance. In effect, only some patches of coating from the inside of the wear track were removed by a deboning mechanism. It is thought that in this case both abrasive and fatigue wear takes place. Also, the Si<sub>3</sub>N<sub>4</sub> sphere used as the counter facing wear component wears significantly in this case. This gradual increase in the contact area resulted in a reduction of the contact stresses acting on the coating. As the contact pressure is reduced, there is a marked reduction in abrasive wear, until the coating eventually fails by fatigue.

### 3.7 Corrosion resistance of AM50 substrates, coated with various thickness

The evaluation of the corrosion resistance of the coated magnesium samples was conducted using the acidified saline solution immersion test developed by General Motors, B.L. Taiwari and J. J. Bommarito [40]. In another publication a similar setup was designed to conduct potentiodynamic tests on the coated surface [34]. For these tests, the coated area of the specimen acts as the working electrode of the potentiostat. For this series of experiments four coating systems were selected. The RIBAD TiN and IBAD Al<sub>2</sub>O<sub>3</sub> for their good wear resistance, and IBSD Ti<sub>x</sub>O<sub>y</sub> and Al<sub>2</sub>O<sub>3</sub> for their good corrosion resistance. Three coating thickness of each were deposited, namely 1μm, 3μm, and 5μm. Figure n.3.11 summarises the results of 48 hours immersion tests, using acidified 5%NaCl solution at PH6. It is immediately apparent, that, the corrosion resistance increases with coating thickness. 1μm and 3μm of RIBAD TiN and IBAD Alumina prove to provide inadequate protection, in fact, magnesium corrosion products are rapidly leached out of the surface and the coating is subsequently detached. Increasing the coating thickness to 5μm results in a substantial improvement, even if, the coatings still show some signs of superficial corrosion damage.



Figure n.3.12 is a plot of the weight loss ratio of coated samples, relative to that of the uncoated substrate material. From this chart, it can be concluded, that for all the various thickness investigated, TiN coatings have a negative influence on the corrosion resistance of the substrate. It can also be seen that at 1µm thickness, the corrosion damage on a TiN coated sample is 2.8 times that of the corresponding uncoated material. In comparison, 1µm IBSD  $Ti_xO_y$  and 1µm IBAD  $Al_2O_3$  do not affect the corrosion process. Figure 4.49 shows small pinholes on the surface of a 3µm RIBAD TiN coating. These defects result in visible damage in the coating, even after just 30min of immersion.

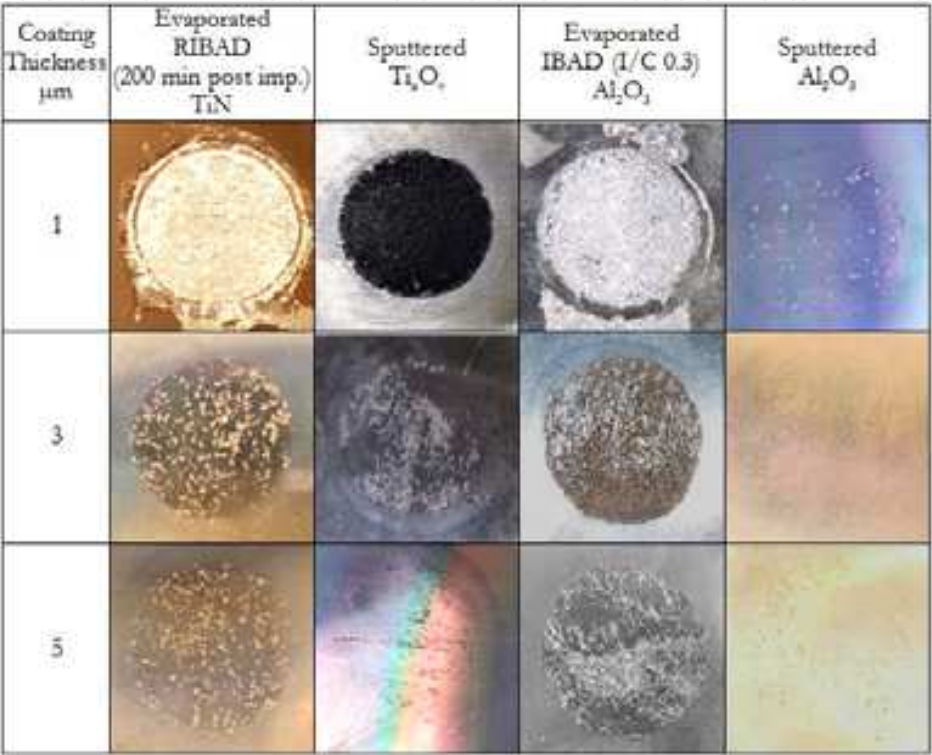


Fig. n.3.10. Showing extent of surface damage following immersion of the various coated substrate in acidified 5% NaCl solution at PH 6 and 20°C for 48 hours.

The corrosion protection of all coatings improves with coating thickness. This is in agreement with the results published by Hollstein *et.al.* [41] maintain that TiN coatings, with a thickness lower than 4µm are not suitable to protect Mg and its alloys from corrosion. Moreover, the results published by this group demonstrate, that single layered TiN coatings have very high porosity. The performance of 1µm IBSD  $Al_2O_3$  is, surprisingly, better than the IBSD  $Ti_xO_y$  coating of the same thickness, and even, better than that of all other coatings tested, even those that are thicker. This enhanced protection is attributed to two important differences in the deposition parameters. The first, and probably the most important, is the fact that aluminium has a lower melting temperature than titanium, and thus sputtering aluminium at temperature, as low as 30°C, results in a  $T_s/T_m$  ratio of 0.33 [zone II of the structure zone model (SZM)], while that for titanium is only 0.19 (Zone I of the SZM). Besides, aluminium has a higher sputtering yield than titanium; which means, that, with the same ion beam current, the Al metal arrival rate attained during sputter deposition, is higher. The ratio of metal arrival rate to residual gas molecules, though still far from unity, is however, somewhat higher than that attained during the sputtering of Ti.

As mentioned above, operating in zone one of the structure zone model results in a low density coating, with a high porosity density, and hence, inferior corrosion resistance. The lower adhesion of  $Ti_xO_y$  coatings, when compared to the IBSD  $Al_2O_3$ , together with the higher XRD signal yield of the latter, provide further support to this hypothesis.

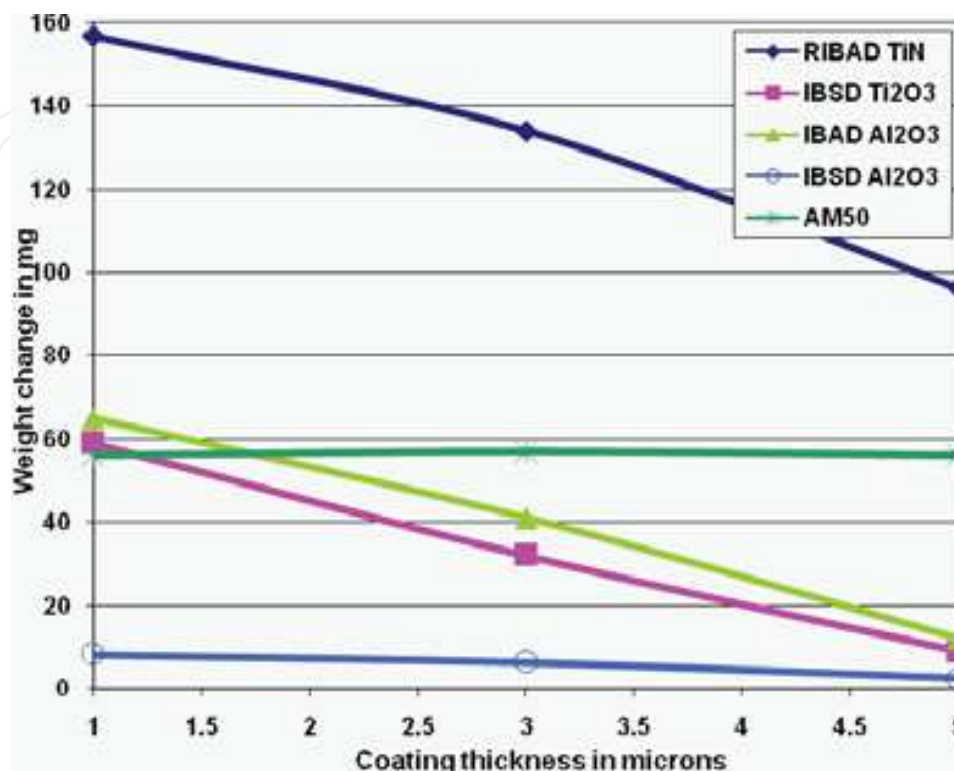


Fig. n.3.12. Weight change of AM50 substrates coated with various thickness and subjected to 48 hours immersion in acidified 5% NaCl solution, following the procedure described in section 3.2.2.4

In the case of IBAD  $Al_2O_3$  coatings, the condensable flux was generated by the electron beam evaporation of aluminium oxide, which resulted in a flux of oxide molecules giving rise to a  $T_s/T_m$  ratio of 0.13. Nevertheless, in this technique, additional kinetic energy is supplied to the growing film by the high energy ion source. Therefore unlike the IBSD coatings, IBAD  $Al_2O_3$  has a high density and hardness. The defects, in this case, originate from high stresses set up by residual gas trapped in the coating and which generate micro cracks and pores. Similar defects in the coating are shown in figure n.3.13. During, the evaporation of the alumina slug within the crucible, globules of alumina may gather charge and be expelled from the crucible, some of which deposit on the sample. Those that remain form inclusions, while those that fall off create pores on the surface, see figure n.3.13. This problem is more prominent at high evaporation rates.

From figure n.3.12, it can be concluded that 5  $\mu m$  IBAD  $Al_2O_3$  coated magnesium substrates perform comparably to the IBSD coatings. However, from Figure n.3.10, it becomes evident that despite the weight loss is similar; the IBAD  $Al_2O_3$  surface is damaged to a greater extent than that of the IBSD coatings. This is believed to be due to the large number of defects present, many of which are smaller than the thickness of the coating. Therefore, this standoff in performance, between the two coatings, is not likely to take place for longer exposure times. In such case, IBSD coatings are expected to yield better performance.

$\text{Al}_2\text{O}_3$  IBAD coated gravity cast AM50 substrates, perform relatively bad, when compared to their squeeze cast AS21 counterpart. The reason for this dissimilarity is thought to be due to the high porosity present in the former. While treating magnesium alloys, using various commercial surface engineering processes [3] discovered that the porosity in the base metal determines the porosity in the coatings. In fact, he attributes the inferior behaviour of coatings deposited on cast magnesium alloys to those on wrought counterparts, to the presence of pores on the surface.

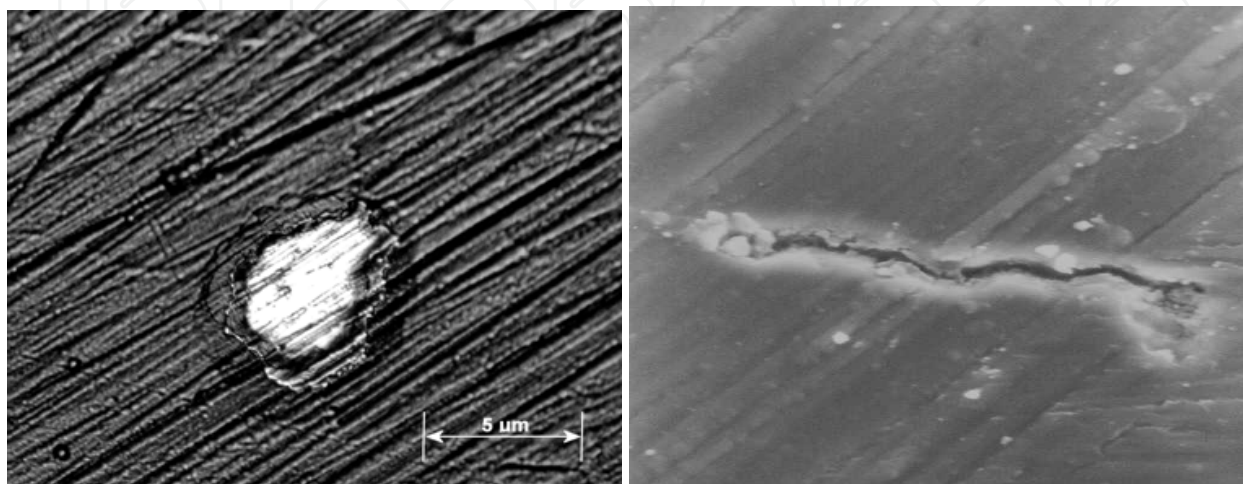


Fig. n.3.13. Left: Pore on IBAD  $\text{Al}_2\text{O}_3$  coating deposited on AM50 substrate, Right: Crack present in the cross section of IBAD on an  $\text{Al}_2\text{O}_3$  coating deposited with an I/C of 0.45.

In the case of the  $1\mu\text{m}$  thick IBAD  $\text{Al}_2\text{O}_3$  coated substrate the active corrosion mechanism is filiform corrosion. This corrosion mechanism operates on surfaces covered with damaged passive coatings. In this case corrosion starts from defects in the coating and propagates underneath the coating producing trenches in the surface. Hoche *et.al.* [31] reported similar corrosion mechanism operating both on  $9\mu\text{m}$  CrN and  $0.5\text{ MgO} + 1.5\mu\text{m}$   $\text{Al}_2\text{O}_3$  coated AZ91 magnesium alloys. While filiform corrosion took place in both cases, the damage experienced on the CrN coated substrate was much greater. This was ascribed to the conductivity of the CrN coating.

S. Korablov *et.al.* [38] explored into the performance of TiN, (Ti,Al)N and CrN PVD coated steel in various aqueous solutions. This investigation showed that nitride coatings can protect the substrate very effectively, in neutral and alkaline solutions. They are, however, rapidly damaged in acidic solution. According to S. Korablov *et.al.*, the nitride coatings are compromised by corrosion products, which initiate at coating defects and spread through the interface causing extensive damage to the coating. This is in net agreement with the findings reported here.

Figure n.3.14 illustrates a series of potentiodynamic tests, conducted on alumina coated substrates, in neutral 5% NaCl solution. In this chart, curve A shows the polarization behaviour of a  $10\mu\text{m}$  IBAD coating on AS21 substrate, while curves B, C, and D show the polarization behaviour of  $1\mu\text{m}$ ,  $5\mu\text{m}$ , and  $15\mu\text{m}$  IBSD coatings deposited on AS21 substrates. At first sight, it is apparent that the free corrosion potential of the  $10\mu\text{m}$  IBAD coating is higher than that of the  $1\mu\text{m}$  thick IBSD coating. Also, the free corrosion potential of IBSD coatings decreases gradually with coating thickness. Still, perhaps, the most important difference in these curves is their lowering of the pitting potential, from  $0.6\text{V}$  to below the

range covered by the potentiostat in use, namely (-2.5V). The vast difference in performance, maybe, can be better appreciated, by comparing the damage produced on the coated surface of the substrates during the polarization experiments.

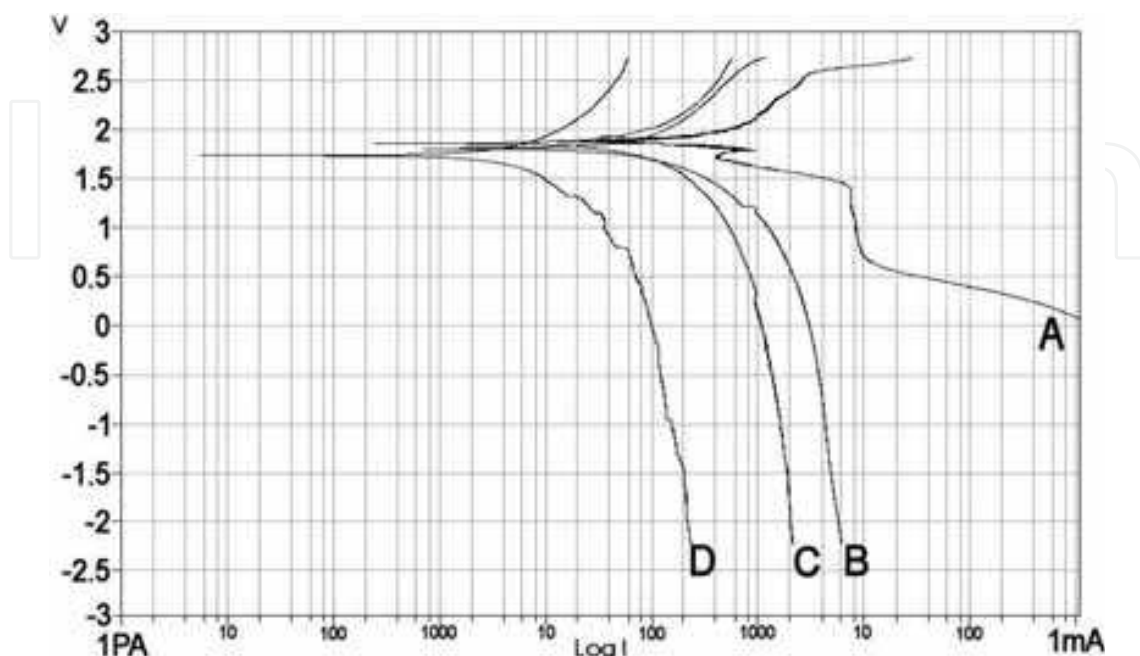


Fig. n.3.14. Potentiodynamic tests on  $\text{Al}_2\text{O}_3$  coated AS21 magnesium alloy. Curve A illustrates the behaviour of the  $10\mu\text{m}$  IBAD  $\text{Al}_2\text{O}_3$ , while plots B, C and D illustrate the behaviour of 5, 10 and  $15\mu\text{m}$  of IBSD  $\text{Al}_2\text{O}_3$ .

From the polarization curve A, it can be seen, that as the sample surface is driven into the anodic region, the current through the defects in the coating increases. At some point, however, this current becomes saturated and further increase in voltage results in very little increase in current. This effect is known as concentration polarization. This corresponds to the dissolution of magnesium through tiny pores in the coating. As corrosion conditions are made more aggressive, the pores grow in diameter and eventually merge to form large pits. This corresponds to a sudden increase in current, which can be observed in curve A at 0.6 volts, and is known as the pitting potential.

From curves B, C, and D of figure n.3.14, it can be seen, that, IBSD alumina coatings do not experience pitting during potentiodynamic tests; through the whole range of polarization voltage used. This is because these coatings have a lower defect concentration, and thus, the pinholes on the surface are further apart than those in the coating represented by curve A. In the former case, therefore, pores cannot merge to form pits or at least, would take much longer to do so. This results in a high resistance to the flow of  $\text{Mg}^{2+}$  out of the surface, which is represented by the steep gradient in the polarization curves for the IBSD coatings.

Hikmet Altun and Sadri Sen <sup>[98]</sup> have conducted extensive potentiodynamic testing of AlN sputter deposited coatings on a range of AZXX magnesium alloys. The coating thickness used for this set of experiment consisted of,  $3\mu\text{m}$  of AlN together with, an Al interlayer of a few nm. The coating provided little protection, to all but one alloy of the series investigated, namely AZ91. For the AlN coated AZ91, the coating provided reasonable good protection with a reported pitting potential a little bit higher than 700mV. Hikmet Altun and Sadri Sen, attribute the limited protection provided by those coatings, to the deposition process related



defects, namely cracks and pores in the coatings. This is in accord with the findings in this research, and those reported by all other researchers mentioned above. The pitting potential for AlN coated AZ91 is reasonable close to that measured on IBAD Alumina coated AS21, produced in this study. The slightly better performance shown in figure n.3.14 (curve A) of the latter is attributable to the higher thickness.

The results obtained in the previously reported immersion tests contrary to those obtained in the potentiodynamic testing. This difference in performance was also observed by F. Stippich *et.al.* [36], while investigating the corrosion protection offered by various magnesium oxide coatings on magnesium alloy substrates. In their study, pure MgO coatings outperformed alloyed MgO and IBAD MgO coatings in potentiodynamic testing. However, they proved inferior during salt spray testing. Stippich *et.al.* concluded that for the purpose of electrochemical testing, greater protection is offered by coatings with amorphous structures, as these have lower porosity. Then again, the mechanical properties of the coatings are more influential in salt spray tests, than in potentiodynamic examination.

#### 4. Conclusion

In the light of the above discussion, it is reasonable to believe that the low ad-atom mobility during sputter deposition resulted in highly amorphous IBSD oxide coatings; with good corrosion resistance but relatively poor mechanical properties, even for coating thickness below 3µm. Conversely, IBAD coatings contain many defects, which lower their resistance to corrosive solutions. These coatings can, however, be substantially improved either by increasing the coating thickness, or by depositing additional coatings with minimal surface porosity. It can also be concluded that conductive coatings, such as, carbon in the form of graphite, titanium nitride and tungsten, can significantly accelerate corrosion by setting up galvanic corrosion. This either results in severe pitting, or filiform corrosion, which will eventually detach the coating completely from the surface.

It was shown that even using conventional hardware developed for the surface engineering of steels, it is possible to deposit coatings that exhibit wear and corrosion resistance onto magnesium alloys. In this study, a hybrid coating was produced by combining the good mechanical properties of IBAD Al<sub>2</sub>O<sub>3</sub>, with the low surface porosity of IBSD C. This resulted in a coating with good overall performance and satisfied the objectives of this project. This work has also served to demonstrate that there is still ample room for improvement, both in the deposition system and ultimately in the protective coatings.

Results published by the various researchers working in this field amply demonstrate that there are two major obstacles for the deposition of dense protective coatings at low temperature. These are the shadowing of the incoming ad-atoms by the shape of the substrate or the texture of its surface and the incorporation of unwanted molecules from the residual gas. The effect of the latter can be easily mitigated by reducing the base and operating pressures, while the former problem is much more difficult to solve. This was traditionally dealt with by incorporating complex substrate manipulators which continually move the substrate surface during deposition in order to expose shadowed features. Unfortunately this approach is not very economical as it requires a large capital expenditure and significantly prolongs the process time. Another problem with these technologies is the inherent delicate nature of the complex equipment used which is prone to very expensive breakdowns.

A more practical approach involves the immersion of the component being treated in the plasma and the application of a pulsed high voltage during deposition, a process known as



Plasma Immersion Ion Implantation & Deposition (PIIID). This comparatively simple solution offers a number of advantages with respect to the more traditional IBAD / RIBAD techniques. The first and most important advantage is that fact that with this technology the energetic charged particles are attracted directly on to the substrate surface. This means that in this case, with very little exceptions the line of sight problem is nonexistent. In addition provided that the sample is properly cooled, the energy density that can be applied on the growing film with this technology is much higher. This means that the condensable flux intensity can be increased without compromising the coating properties resulting in much higher deposition rates. Another important advantage of this setup is the possibility to easily modify the surface of the substrate before deposition. In fact this setup is particularly suitable for the preparation of duplex and multilayer coatings.

Notwithstanding these important advantages it is unlikely that the PIIID technology will ever offer the same degree of process parameter control over the IBAD / RIBAD or the IBSD systems. These are likely to maintain their dominance in specific applications where accurate control of the coating crystal structure is required.

## 5. Reference

- [1] Kondrat'ev S. Yu. , Yaroslavskii G. Ya., & Chaikovskii B. S. (1986). Strength of Materials, Volume 18, number 10 / October, pages 1325 – 1329, Springer US.
- [2] Polmear J. (1995). *Light alloys Metallurgy of light metals, Third edition*, Hodder & Stoughton, ISBN: 0-340-63207-0, Huddersfield, WY, United Kingdom. pg. 196-20
- [3] Michael M. Avedesian & Huge Barker, (1999). *Magnesium and Magnesium Alloys, ASM specialty handbook published by the materials information society*, ISBN: 0-87170-657-1, United States. pg.194–210, 145, 157, & 159.
- [4] Gaines L., Cuenca R., Stodolsky F., & Wu S. (1996). Potential Automotive Uses of Wrought Magnesium Alloys, Automotive Technology Development, Detroit, Michigan.
- [5] Friedrich H. & Schumann S. (2002). Mineral Processing and Extractive Metallurgy: *IMM Transactions section C*, Volume 111, number 2, August, pages 65-71(7).
- [6] Morton P.H. (1992). *Surface engineering and heat treatment, past, present, and future*. Institute of Metals, ISBN: 0901716014, London. pg.12–51
- [7] W. Ensinger (1992). Ion beam assisted deposition with a duoplasmatron, *Review of Scientific Instruments* Volume 63, Issue 4, April, page 2393.
- [8] Bestetti M., Cavallotti P.L., Da Forno, & A.and Pozzi S. (2007). Anodic oxidation and powder coating for corrosion protection of AM60B magnesium alloys, *Transactions of the Institute of Metal Finishing*, Volume 85(6), pages 316- 319.
- [9] Bestetti M., Barlassina F., Da Forno A., & Cavallotti P.L. (2008). Effect of electrolyte composition on micro-arc anodization of AM60B magnesium alloy, *Metallurgical Science and Technology*, Vol. 26-1 - Ed. 2008, Torino, Italy.
- [10] Klingenberg M., Arps J., Wei R., Demaree J., & Hirvonen J. (2002). 'Practical Applications of Ion Beam and Plasma Processing for Improving Corrosion and Wear Protection, *Surface and Coatings Technology* Volumes 158-159, September, Pages 164-169.
- [11] Arnold H. Deutchman & Robert J. Partyka, (2002). Ion Beam Enhanced Deposited (IBED) Tribological Coatings for Non-Ferrous Alloys, *Proceedings from the 1st*

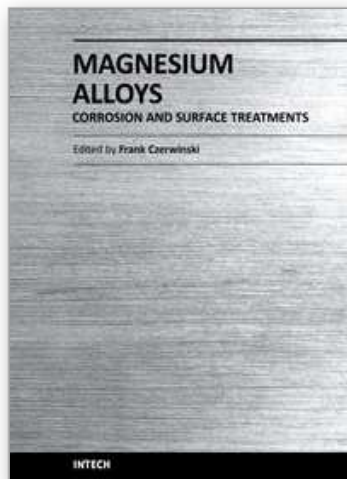
- International Surface Engineering Congress and the 13<sup>th</sup> IFHTSE Congress*, 7-10 October, Columbus Ohio, USA.
- [12] Tadatsugu Itoh, (1989). *Beam Modification of Materials 3. Ion Beam Assisted Growth*. Elsevier, ISBN: 0444872809, Amsterdam and New York. pg.170-179
  - [13] Arnold H. Deutchman, & Robert J. Partyka, (2002). 'Comparison of the Properties of PVD and IBED Hardcoats (TiN and Cr<sub>2</sub>N)', *Proceedings from the 1st International Surface Engineering Congress and the 13th IFHTSE Congress*, 7-10 October, Columbus Ohio, USA.
  - [14] Shin-Hui Wang, Ching-Chun Chang, & J. S. Chen, (2004). Effects of substrate bias and nitrogen flow ratio on the resistivity, density, stoichiometry, and crystal structure of reactively sputtered ZrN<sub>x</sub> thin films, *Journal of Vacuum Science and Technology A: Vacuum, Surfaces, and Films*, Volume 22, Issue 5, September, pages 2145-2151.
  - [15] Emmerich R., Enders B., & Ensinger W. (1992). Ion beam assisted deposition of thin films and coatings: Part 1, *Surface Modification Technologies VI, Proceedings of the Sixth International Conference on Surface Modification Technologies*, Chicago USA, Novemb, ISBN: 0-87339-217-5.
  - [16] André Anders, (2000). *Handbook of Plasma Immersed Ion Implantation and Deposition*. Published by wiley-interscience, New York, ISBN: 0-471-24698-0. pg.177-209
  - [17] Mändl S., Brutscher J., Günzel R., and Höller W. (1996). Design Considerations for Plasma Immersion Ion Implantation Systems, *Nuclear instruments and methods in physics research B*, Volume 112, , pages 252-254. [27]
  - [18] Emmerich R., Enders B., & Ensinger W. (1992). Ion beam assisted deposition of thin films and coatings: part 2, *Surface Modification Technologies VI, Proceedings of the Sixth International Conference on Surface Modification Technologies*, Chicago USA, Novemb, November 2-5, ISBN: 0-87339-217-5.
  - [19] Enders B., Emmerich R., & Ensinger W. (2000). Ion beam assisted deposition under off-normal ion incidence: an experimental and analytical study of re-sputtering effects, *Surface and Coatings Technology* Volumes 128-129, 1 June, Pages 303-307.
  - [20] Emmerich R., Enders B., & Ensinger W. (1992). Ion beam assisted deposition of thin films and coatings: part 3, *Surface Modification Technologies VI, Proceedings of the Sixth International Conference on Surface Modification Technologies*, Chicago USA, Novemb, ISBN: 0873392175.
  - [21] Hopf C., Jacob W., & von Keudell A. (2005). Ion-induced Surface Activation, Chemical Sputtering, and Hydrogen Release during Plasma-assisted Hydrocarbon Film Growth, *Journal of Applied Physics*, volume 97, number 9, pages 094904.1-094904.6
  - [22] Müller K.H., & Karl-Heinz. (1987) (Date of Current Version: 07 July 2009). Stress and microstructure of sputter-deposited thin films: molecular dynamics investigations, *Journal of Applied Physics*, Volume 62, issue 5, ISSN: 0021-8979. pages 1796-1799.
  - [23] Valvoda B. (1996). Structure of TiN coatings, *Surface and coatings technology*, volume 80, no 1-2, pages 61 - 65.
  - [24] Kiyotaka Wasa & Shigeru Hayakawa, (1992). *Handbook of Sputter Deposition Technology principles technology and applications*, Noyes publications, Berkshire. RG12 8DW. UK, ISBN: 0-8155-1280-5. pg.65-78

- [25] Hua M. , Ma H.Y. , Mok C.K. , & Li J. (2004). Tribological Behavior of Patterned PVD TiN Coatings on M2 Steel, *Jurnal of Tribology letters*, Volume 17, Number 3, pages 645-653.
- [26] Gao Chum, Malmhall Roger, & Chen Ga-Lane, (1997). Quantitative characterization of sputter-process-induced nano-voids and porous film state in magnetic thin films, *IEEE transactions on magnetics*, volume 33, no. 5, ISSN: 0018-9464, pages 3013-3015.
- [27] Konczos G., Bársony I. & Deák P. with the support of the Tempus Sjep 09614-95, (1998). *Introduction to materials science and technology*. A textbook of the technical university of Budapest. For the P.hD. students in physics. Chapter 5
- [28] Ignatenko P. I., Klyakhina N. A., & Badekin M. Yu. (2005). Structure and properties of films grown on Si, Ta, Ti, Mo, W, and Ni substrates by reactive ion-beam sputtering, *Jurnal of Inorganic Materials*, Vol. 41, number 2, pp. 148-151. Translated from *Neorganicheskie Materialy*, Vol. 41, number 2, 2005, pp. 193-196.
- [29] Petrov I., Brana P.B., Hultman H., & Greene J.E. (2003). Microstructural evolution during film growth, *Jurnal of Vacuum Science and Technology A*, Volume 21, number 5, September-October, ISSN: 0734-2101 , Page(s): S117 - S128.
- [30] Busk R.S. (1987). Magnesium and its alloys, *International Magnesium Association* 1987, Hilton Head, South Carolina, pages S497-S499.
- [31] Hoche H., Scheerer H., Probst D., Broszeit E., & Berger C. (2003). Development of a plasma surface treatment for magnesium alloys to ensure sufficient wear and corrosion resistance, Proceedings of the Eight International Conference on Plasma Surface Engineering, *Surface and coating technology*, Volume 174-175, Pages 1018-1023.
- [32] Hoche H., Blawert C., Broszeit E., & Berger C. (2005). Galvanic corrosion properties of differently PVD-treated magnesium die cast alloy AZ91, proceedings from teh Asian-European International Conference on Plasma Surface Engineering 2003, *Surface and Coating Technology*, Volume 193, pages 223-229.
- [33] Nuno Jorge and Carvalho Marcolino, (2001). *Lower friction and wear resistant coatings. Microstructure and mechanical properties*. Groningen University Press, Netherlands, ISBN 90 367 1378 1.
- [34] Dong H. (2010). *Surface engineering of light alloys*, CRC press, woodheadpublishing uk, ISBN 1 84569 537 2. Pg. 307
- [35] Kurth M., Graat P. C. J., Carstanjen H. D., & Mittemeijer E. J. (2006). The initial oxidation of magnesium: an *in situ* study with XPS, HERDA and ellipsometry, *Surface and Interface Analysis*, Volume 38, Pages 931-940.
- [36] Stippich F., Vera E., Wolf G. K., Berg G., & Friedrich Chr. (1998). Enhanced corrosion protection of magnesium oxide coatings on magnesium deposited by ion beam-assisted evaporation, *Surface and Coatings Technology*, Volume 103-104, pages 29-35.
- [37] Vander G. F. Voort, (2006). *ASM Handbook, Volume 9. Metallography and Microstructures*. ISBN: 0-87170-706-3. pg.1061-1062
- [38] Korablov S., Basavalingu B. & Yoshimura M. (2005). Wet corrosion of nitride PVD films in supercritical solutions, *Corrosion Science*, Volume 47, Issue 6, pages 1384-1402.
- [39] Clarke D.R. & Pompe W. (1999). Critical radius for interface separation of a compressively stressed film from a rough surface, *Acta Materialia*, Volume 47, Number 6, pages 1749-1756(8).

- [40] Taiwari B.L. & Bommarito J. J. (2002). A novel technique to evaluate the corrosion behaviour of magnesium alloys, *General Motors R&D Center, Kaplan, HI editor, Magnesium Technology*, TMS, Warrendale, PA, pages 269-275.
- [41] Hollstein Frank, Wiedemann Renate, & Scholz Jana (2003). *Characteristics of PVD-coatings on AZ31hp magnesium alloys*, Surface and Coating Technology, Volume 162, pages 261-268.

IntechOpen

IntechOpen



## **Magnesium Alloys - Corrosion and Surface Treatments**

Edited by Frank Czerwinski

ISBN 978-953-307-972-1

Hard cover, 344 pages

**Publisher** InTech

**Published online** 14, January, 2011

**Published in print edition** January, 2011

A resistance of magnesium alloys to surface degradation is paramount for their applications in automotive, aerospace, consumer electronics and general-purpose markets. An emphasis of this book is on oxidation, corrosion and surface modifications, designed to enhance the alloy surface stability. It covers a nature of oxides grown at elevated temperatures and oxidation characteristics of selected alloys along with elements of general and electrochemical corrosion. Medical applications are considered that explore bio-compatibility of magnesium alloys. Also techniques of surface modifications, designed to improve not only corrosion resistance but also corrosion fatigue, wear and other behaviors, are described. The book represents a valuable resource for scientists and engineers from academia and industry.

### **How to reference**

In order to correctly reference this scholarly work, feel free to copy and paste the following:

Stephen Abela (2011). Protective Coatings for Magnesium Alloys, Magnesium Alloys - Corrosion and Surface Treatments, Frank Czerwinski (Ed.), ISBN: 978-953-307-972-1, InTech, Available from:  
<http://www.intechopen.com/books/magnesium-alloys-corrosion-and-surface-treatments/protective-coatings-for-magnesium-alloys>

**INTech**  
open science | open minds

### **InTech Europe**

University Campus STeP Ri  
Slavka Krautzeka 83/A  
51000 Rijeka, Croatia  
Phone: +385 (51) 770 447  
Fax: +385 (51) 686 166  
[www.intechopen.com](http://www.intechopen.com)

### **InTech China**

Unit 405, Office Block, Hotel Equatorial Shanghai  
No.65, Yan An Road (West), Shanghai, 200040, China  
中国上海市延安西路65号上海国际贵都大饭店办公楼405单元  
Phone: +86-21-62489820  
Fax: +86-21-62489821



© 2011 The Author(s). Licensee IntechOpen. This chapter is distributed under the terms of the [Creative Commons Attribution-NonCommercial-ShareAlike-3.0 License](https://creativecommons.org/licenses/by-nc-sa/3.0/), which permits use, distribution and reproduction for non-commercial purposes, provided the original is properly cited and derivative works building on this content are distributed under the same license.

IntechOpen

IntechOpen